

# Quartet Tomography in Multiterminal Josephson Junctions

David Christian Ohnmacht,<sup>1,\*</sup> Marco Coraiola,<sup>2</sup> Juan José García-Esteban,<sup>1,3</sup>  
Deivid Sabonis,<sup>2</sup> Fabrizio Nichele,<sup>2</sup> Wolfgang Belzig,<sup>1</sup> and Juan Carlos Cuevas<sup>1,3,†</sup>

<sup>1</sup>*Fachbereich Physik, Universität Konstanz, D-78457 Konstanz, Germany*

<sup>2</sup>*IBM Research Europe—Zurich, Säumerstrasse 4, 8803 Rüschlikon, Switzerland*

<sup>3</sup>*Departamento de Física Teórica de la Materia Condensada and Condensed Matter Physics Center (IFIMAC),  
Universidad Autónoma de Madrid, E-28049 Madrid, Spain*

(Dated: December 1, 2023)

We investigate the detection of quartets in hybrid multiterminal Josephson junctions. Using simple models of quantum dots coupled to superconducting leads, we find that quartets are ubiquitous and show how to rigorously extract their contribution to the current-phase relation (CPR). We also demonstrate that quartets are closely related to the hybridization of Andreev bound states (ABSs) in these systems and propose a method to identify quartets directly in ABS spectra. We illustrate our method by analyzing the spectroscopic measurements of the ABS spectrum in a three-terminal Josephson junction realized in an InAs/Al heterostructure. Our analysis strongly suggests the existence of quartets in the studied hybrid system.

*Introduction.*— A junction with a short normal conducting region between two superconductors accommodates ABSs which carry a supercurrent through the system [1, 2]. A unique aspect of ABSs lies in the tunability of their energies by changing the superconducting phase difference, which has led to the proposal of ABSs as a platform for quantum computing [3–6]. Additionally, there have been numerous studies reporting on the CPR and the energy spectra of ABSs in two-terminal Josephson junctions (JJs) [7–21]. In multiterminal JJs (MTJJs), the ABSs energies depend on multiple phase differences, enabling band structure engineering which is of particular interest for realizing topological systems [22–35].

MTJJs exhibit a plethora of unique transport phenomena. For instance, in a three-terminal device the commensuration of voltages at two terminals induces dc supercurrents at finite bias, known as voltage-induced Shapiro steps [36]. The same signature was predicted to be related to a transport mechanism referred to as quartet process, which involves one Andreev reflection at terminal  $i$  and  $j$ , respectively, and two crossed Andreev reflections at terminal  $k$ , resulting in a dependence of the supercurrent on a combination of phases given by  $\varphi_i + \varphi_j - 2\varphi_k$  (where  $\varphi_\alpha$  indicates the superconducting phase of terminal  $\alpha$ , for  $\alpha = i, j, k$ ) [37, 38]. Additional theoretical work has proposed strategies to identify quartets both in the current-voltage characteristics [39–48] and in the supercurrent [49, 50]. Following experimental studies resulted in the observation of potential signatures of these processes obtained by probing the system response as a function of two bias currents or voltages [51–54]. Other experiments in hybrid MTJJs, not specifically designed to detect quartets, have also reported signatures compatible with their existence [55–60]. A related system, based on two JJs in proximity of each other, has been proposed to realize Andreev molecules, where hybridization of ABSs occurs [61–64]. In this case, signs of a unconventional coupling mechanism have been pre-

dicted and they have been investigated via current-bias measurements [59, 65, 66]. In addition, spectroscopic evidence of ABS hybridization was recently reported in a hybrid three-terminal JJ, where ABS spectra were probed as a function of two phase differences [67]. However, despite all experimental efforts and theoretical predictions, the unambiguous detection of quartet processes is still a challenge.

In this Letter, we present a scheme which we term *Quartet Tomography* to rigorously extract the quartet contributions from either the CPR or the ABS spectrum of a MTJJ. We apply this scheme to recent measurements of the ABS spectrum of a three-terminal JJ realized in an InAs/Al heterostructure [67] and demonstrate the existence of quartet processes in these MTJJs. Additionally, we show that the quartet contributions are intimately related to the degree of hybridization of the ABSs in these heterostructures and that ABS hybridization is a sufficient, but not necessary condition for the existence of quartet processes.

*Quartet Tomography: single-dot model.*— To illustrate the idea of quartets and how they show up in the CPR of a MTJJ we consider the model illustrated in Fig. 1(a), where a single noninteracting quantum dot is coupled to  $N$  superconducting leads. The quantum dot has a single spin-degenerate level of energy  $\epsilon_0$  and the superconducting electrodes are  $s$ -wave superconductors characterized by energy gaps  $\Delta_j$  and superconducting phases  $\varphi_j$  ( $j = 1, \dots, N$ ). The coupling between the dot and lead  $j$  is described by the tunneling rate  $\Gamma_j$ . Our goal is to compute the supercurrent flowing in the terminals of this system as a function of the phases  $\varphi_j$ . For this purpose, we employ Green’s function techniques and our input are the (dimensionless) retarded and advanced Green’s functions of the leads, which in a  $2 \times 2$  Nambu representation read  $\hat{g}_j^{r/a}(E) = g_j^{r/a} \hat{\tau}_0 + f_j^{r/a} e^{i\varphi_j} \hat{\tau}_3 \hat{\tau}_1$ , with  $g_j^{r/a} = -(E \pm i\eta) / \sqrt{\Delta_j^2 - (E \pm i\eta)^2}$  and  $f_j^{r/a} =$

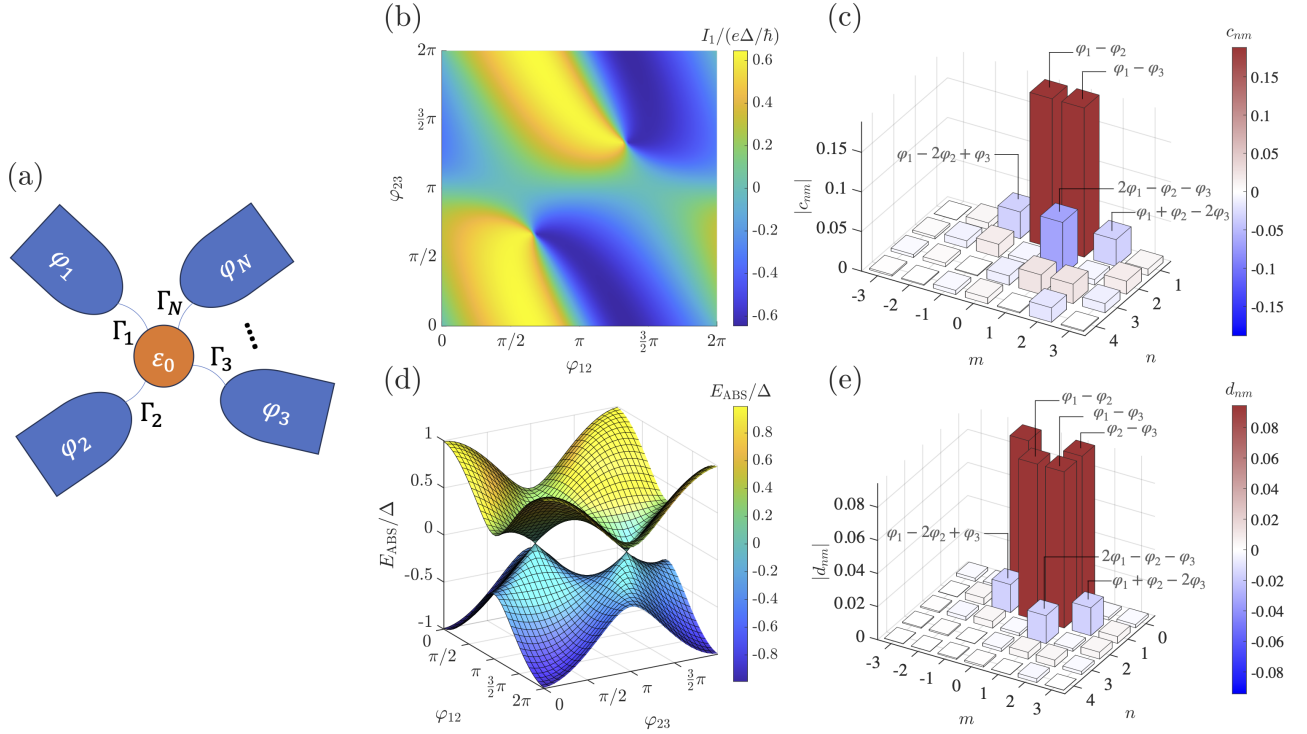


FIG. 1. (a) Schematics of the single-dot model. A single-level quantum dot is coupled to  $N$  superconducting terminals with phases  $\varphi_j$ . The parameter  $\Gamma_j$  describes the strength of the coupling between the dot and lead  $j$ . (b) Example of the current-phase relation  $I_1(\varphi_{12}, \varphi_{23})$  for the model in (a) with three identical leads with energy gap  $\Delta$ . The different parameters are:  $\Gamma_1 = \Gamma_2 = \Gamma_3 = 5\Delta$  and  $\epsilon_0 = 0$ . (c) The corresponding  $c_{nm}$  coefficients in the expansion of Eq. (3) in units of  $e\Delta/\hbar$ . The phase dependence associated to some of these coefficients is indicated in the graph. (d) Andreev bound state spectrum  $E_{\text{ABS}}(\varphi_{12}, \varphi_{23})$  for the example shown in panel (b). (e) The corresponding  $d_{nm}$  coefficients in the expansion of Eq. (6) in units of  $\Delta$ .

$-\Delta_j/\sqrt{\Delta_j^2 - (E \pm \eta)^2}$ . Here,  $E$  is the energy,  $\eta = 0^+$ , and  $\tau_{0,1}$  are Pauli matrices. As we show in the Supplemental Material [68], one can express the current flowing through lead  $i$  as  $I_i = \sum_{j \neq i} I_{ij}$ , where  $I_{ij}$  is given by

$$I_{ij} = \frac{8e}{h} \Gamma_i \Gamma_j \sin(\varphi_{ji}) \int_{-\infty}^{\infty} \Im \left\{ \frac{f_i^a(E) f_j^a(E)}{D(E, \vec{\varphi})} \right\} n_F(E) dE. \quad (1)$$

Here,  $\varphi_{ij} = \varphi_i - \varphi_j$ ,  $n_F(E)$  is the Fermi function,  $\vec{\varphi} = (\varphi_1, \dots, \varphi_N)$ , and  $D(E, \vec{\varphi})$  is given by

$$D(E, \vec{\varphi}) = \left[ E - \epsilon_0 - \sum_k \Gamma_k g_k^a \right] \left[ E + \epsilon_0 - \sum_k \Gamma_k g_k^a \right] - \left[ \sum_k \Gamma_k f_k^a e^{i\varphi_k} \right] \left[ \sum_k \Gamma_k f_k^a e^{-i\varphi_k} \right]. \quad (2)$$

The ABS energies in this structure are derived from the condition  $D(E, \vec{\varphi}) = 0$ .

We focus now on a three-terminal device and consider the current  $I_1$ . This current depends on two phase differences, chosen  $\varphi_{12} = \varphi_1 - \varphi_2$  and  $\varphi_{23} = \varphi_2 - \varphi_3$ , and can be expressed as the Fourier series:

$$I_1(\varphi_{12}, \varphi_{23}) = \sum_{n,m} c_{nm} \sin(n\varphi_{12} + m\varphi_{23}), \quad (3)$$

with  $c_{0m} = 0$ , namely there are no contributions of the type  $\sin(\varphi_2 - \varphi_3)$ , and  $c_{nm} = -c_{-n-m}$ .

In this system, a quartet is a correlated Cooper pair tunneling process that involves three terminals and whose contribution to the supercurrent depends on a phase of the type  $\varphi_k^q = \varphi_i + \varphi_j - 2\varphi_k$  with  $i, j \neq k$  and  $i \neq j$ . There are three types of quartets, and from Eq. (1) one can show that the corresponding contributions to leading order in the  $\Gamma$  parameters are given by [68]:  $c_{-2,-1} = 2Q_1$ ,  $c_{1,-1} = -Q_2$ ,  $c_{1,2} = -Q_3$ , where

$$Q_k = \frac{8e}{h} \Gamma_i \Gamma_j \Gamma_k^2 \int_{-\infty}^{\infty} dE n_F(E) \times \Im \left\{ \frac{f_i^a(E) f_j^a(E) [f_k^a(E)]^2}{(E^2 - \epsilon_0^2)^2} \right\}. \quad (4)$$

Equation (4) supports the interpretation that a quartet of the type  $\varphi_1^q = \varphi_2 + \varphi_3 - 2\varphi_1$  involves the injection of two Cooper pairs from terminal 1 that are transferred separately to leads 2 and 3. Let us emphasize that the supercurrent  $I_1(\varphi_{12}, \varphi_{23})$  contains not only quartet contributions of the kind  $\sin(\varphi_k^q)$ , but also harmonics of this phase. More importantly, Eq. (3) suggests a direct way to extract the quartet contributions, which consists in performing a Fourier analysis of the CPR. We illustrate the

results for this model in Fig. 1 where we show both the CPR  $I_1(\varphi_{12}, \varphi_{23})$  in panel (b) and the  $c_{nm}$  coefficients in the expansion of Eq. (3) in panel (c). We note the appearance of the three types of quartet contributions predicted above, see panel (c). Moreover, as expected from Eq. (4) for a symmetric situation (all  $\Gamma$ 's and  $\Delta$ 's equal), the quartet  $\varphi_1^q$  has a magnitude that is twice that of the other two,  $\varphi_2^q$  and  $\varphi_3^q$ , while it contributes to the current  $I_1$  with an opposite sign. It is worth stressing that quartet contributions are accompanied by other, more dominant contributions related to terms proportional to  $\sin(\varphi_{ij})$  and their harmonics. Those additional contributions originate from the tunneling of single and multiple Cooper pairs, respectively (see Ref. [68]). Their unavoidable presence complicates the identification of quartets in the analysis of transport properties such as the critical current. This problem is resolved by our quartet tomography because it does not rely on the relative magnitude of the different contributions.

*ABS energies and supercurrent.*— As we have just shown, quartets are easily identified from the CPR. However, to isolate the CPR of one terminal in a phase-controlled MTJJ is challenging. For this reason, we propose a second method based on the measurement of the density of states (DOS) by means of tunneling spectroscopy like in Ref. [67]. From the DOS we can deduce the ABS spectrum, which in turn is closely related to the supercurrent. In fact, in short coherent structures with a junction length smaller than the superconducting coherence length, the supercurrent is completely carried by the ABSs. In our MTJJ, the zero-temperature current  $I_1$  is obtained from the energies  $E_{\text{ABS}}^{(l)}$  of the occupied ABSs as follows

$$I_1(\vec{\varphi}) = \frac{2e}{\hbar} \sum_l \frac{\partial E_{\text{ABS}}^{(l)}(\vec{\varphi})}{\partial \varphi_1}. \quad (5)$$

The factor 2 appears because we are assuming spin degeneracy. We have verified that, in the examples shown in this work, we can reconstruct the CPR using Eq. (5). This demonstrates that the supercurrent is carried by the ABSs with no contributions from the continuum. Therefore, there is an even simpler protocol to identify quartets, which consists in the Fourier analysis of the ABS spectrum. In the case of a three-terminal junction, this spectrum admits a Fourier expansion of the type:

$$E_{\text{ABS}}^{(l)}(\vec{\varphi}) = - \sum_{nm} d_{nm}^{(l)} \cos(n\varphi_{12} + m\varphi_{23}). \quad (6)$$

The Fourier coefficients  $d_{nm}^{(l)}$  are related to the Fourier coefficients of the supercurrent via Eq. (5). The results for the energy of the occupied and unoccupied ABS for the single-dot model are shown in Fig. 1(d). These two states touch at zero energy in this example because, for our choice of parameters, the ABSs have perfect transmission. The corresponding Fourier components for the

occupied ABS are displayed in panel (e). Here, the color indicates whether a contribution is positive or negative, whereas the bar height is a measure of its absolute value. Notice that quartet contributions are clearly visible and in accordance with the Fourier components of the CPR in Fig. 1(c). Note also that the coefficient  $d_{00}$  is not shown because it does not contribute to the supercurrent.

*Quartets and ABS hybridization: double-dot model.*— Since quartets are correlated tunneling events involving three terminals, they are closely related to the hybridization of ABSs in these structures. To illustrate this idea we now consider the double quantum dot model illustrated in Fig. 2(a). This model was recently used to describe the hybridization of ABSs in Ref. [67] (see below). In this case, the normal scattering region is formed by two single-level quantum dots (with energies  $\epsilon_1$  and  $\epsilon_2$ ). These dots are coupled to three superconducting terminals as shown in Fig. 2(a). There is an interdot coupling described by the parameter  $t$ , which controls the degree of hybridization of the ABSs. Again, using Green's function techniques one can compute the supercurrent that flows through the different terminals; the details are presented in Ref. [68]. Crucially, the current  $I_1$  admits the same Fourier expansion of Eq. (3). A perturbative analysis shows that one has the same three types of quartets as in the single-dot model, and all contributions have a similar form. For instance, for the quartet  $\varphi_3^q = \varphi_1 + \varphi_2 - 2\varphi_3$ , we obtain a contribution to the current of the form  $Q_3 \sin(\varphi_3^q)$ , where  $Q_3$  is given to leading order in  $t$  and the  $\Gamma$  parameters [see Fig. 2(a)] by

$$Q_3 = \frac{8e}{\hbar} t^2 \Gamma_1 \Gamma_3^2 \int_{-\infty}^{\infty} dE n_{\text{F}}(E) \times \quad (7)$$

$$\Im \left\{ \frac{f_1^{\text{a}}(E) f_2^{\text{a}}(E) [f_3^{\text{a}}(E)]^2}{(E^2 - \epsilon_1^2)(E^2 - \epsilon_2^2)} \left( \frac{\Gamma_{2,1}}{E^2 - \epsilon_1^2} + \frac{\Gamma_{2,2}}{E^2 - \epsilon_2^2} \right) \right\}.$$

This expression shows that quartets would not be possible without ABS hybridization, as  $Q_3$  vanishes for zero interdot coupling ( $t = 0$ ).

We illustrate the results for this model in Fig. 2(b,c) where we show an example of the energy of the highest occupied ABS,  $E_{\text{ABS}}^{(1)}(\varphi_{12}, \varphi_{23})$ , along with the  $d_{nm}^{(1)}$  coefficients in the expansion of Eq. (6) (see caption for parameter values). Hybridization signs of the ABSs connecting the pairs of terminals 1-2 and 2-3 are clearly visible in the region  $(\varphi_{12}, \varphi_{23}) \sim (\pi, \pi)$ , where the ABS energy differs from that of the two independent states. More importantly, this hybridization gives rise to three quartet contributions, which again are accompanied by terms that involve phase differences between only two terminals. The close relation between quartets and ABS hybridization is further explored in Ref. [68].

*Quartet Tomography in a three-terminal Josephson junction.*— The two protocols described above to identify quartet contributions can be directly applied to experimental data. We now illustrate this with the analysis of

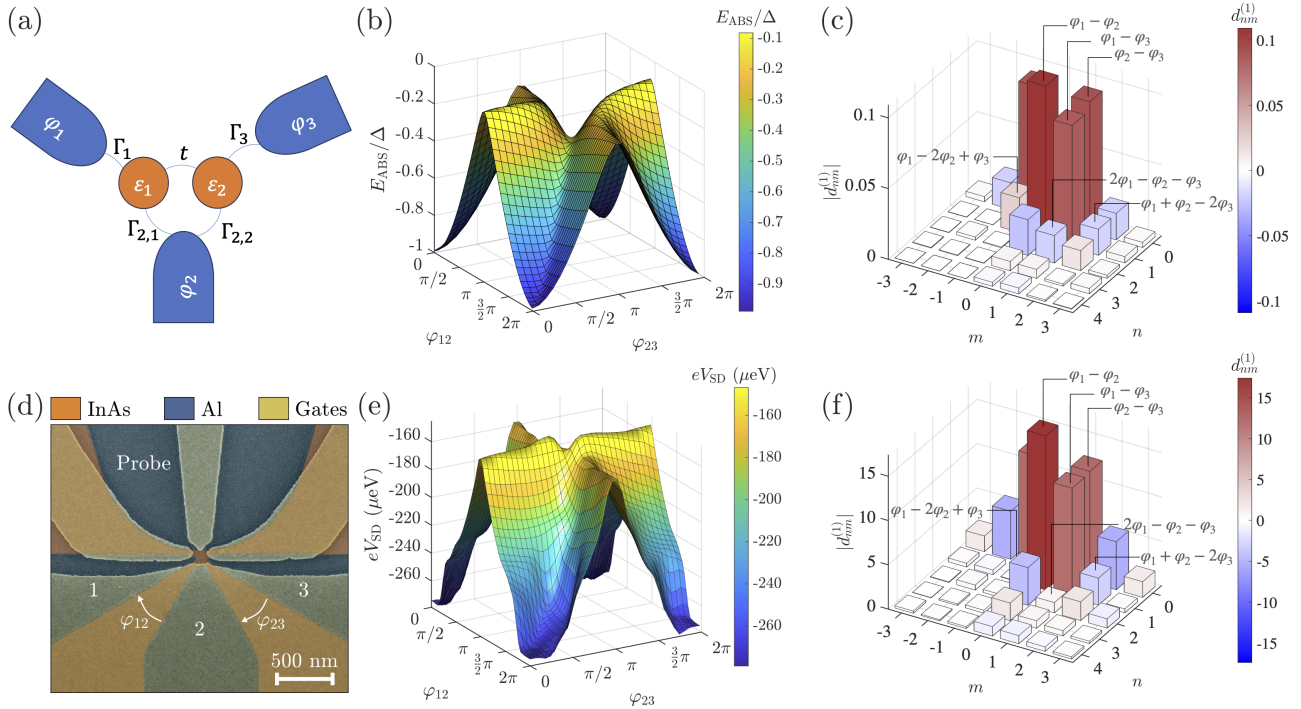


FIG. 2. (a) Schematics of the double-dot model. (b) Example of the energy  $E_{\text{ABS}}^{(1)}(\varphi_{12}, \varphi_{23})$  of the highest occupied ABS in the model of panel (a). The different parameters are:  $\Delta_{1,2,3} = \Delta$ ,  $\Gamma_1 = 5.5\Delta$ ,  $\Gamma_{2,1} = 6\Delta$ ,  $\Gamma_{2,2} = 5\Delta$ ,  $\Gamma_3 = 6\Delta$ ,  $t = 5\Delta$ , and  $\epsilon_1 = \epsilon_2 = 0$ . (c) The corresponding  $d_{nm}^{(1)}$  coefficients in the expansion of Eq. (6) measured in units of  $\Delta$ . The phase dependence associated to some of these coefficients is indicated in the graph. (d) False-colored scanning electron micrograph of the device measured in Ref. [67], near to the three-terminal Josephson junction region. Exposed semiconductor is shown in orange, aluminum in blue and gate electrodes in gold. (e) The upper ABS extracted from the tunneling spectroscopy data of Ref. [67], where  $V_{\text{SD}}$  is the bias voltage applied to the superconducting probe. (f) The corresponding  $d_{nm}^{(1)}$  coefficients of Eq. (6) in  $\mu\text{eV}$  that show the presence of quartets in the studied device.

the quartet contributions in the ABS spectrum measured in Ref. [67]. The device investigated in that work, shown in Fig. 2(d), consisted of three superconducting terminals (Al) coupled to a normal region (InAs). Terminals 1 and 2 (2 and 3) were connected to form a closed loop, hence enabling control over the phase difference  $\varphi_{12}$  ( $\varphi_{23}$ ) via integrated flux-bias lines. The DOS in the normal region was probed via tunneling spectroscopy, performed by applying a voltage bias  $V_{\text{SD}}$  to a fourth superconducting terminal. Further details about materials, fabrication and measurements can be found in Ref. [67]. Using the information of the tunneling spectra as a function of the two phase differences and with the help of a deep learning algorithm [68], we reconstructed the phase dependence of the highest occupied ABS in this device, see Fig. 2(e). Notice that the ABS spectrum is presented in terms of the probe voltage and thus, it is offset by the gap of the superconducting probe [67], which has no influence in the tomography. From this ABS spectrum, and using the protocol described above, we obtained the coefficients of the quartet tomography  $d_{nm}^{(1)}$  that are shown in Fig. 2(f). Again, the coefficient  $d_{00}^{(1)}$  is not shown. Notice that the quartet contributions  $d_{12}^{(1)}$  and  $d_{21}^{(1)}$  related to

the phases  $\varphi_3^q$  and  $\varphi_1^q$ , respectively, have a relatively large magnitude resulting in a sizeable quartet contribution to the supercurrent. This is a consequence of the significant ABS hybridization in this device, which is clearly visible in the region  $(\varphi_{12}, \varphi_{23}) \sim (\pi, \pi)$  and whose signatures were amply discussed in Ref. [67]. This issue is further addressed in Ref. [68], where we also present an analysis illustrating the robustness of the quartet tomography.

*Conclusions.*— We have put forward two protocols to identify quartets in multiterminal Josephson junctions. In particular, we have shown how quartet contributions can be extracted from measurements of the ABS spectrum of a three-terminal hybrid Josephson junction [67]. We have also shown that in heterostructures featuring several ABSs, as it is normally the case, quartets are intimately related to the hybridization of ABSs. It is worth stressing that the protocol based on the analysis of the CPR could, in principle, be used to identify quartets in CPR measurements in Andreev molecules [65, 66]. From a theoretical point of view, it would be interesting, among other things, to study the connection between quartets and topological states, as well as to investigate the impact of the spin-orbit interaction in these correlated tunneling

events [69, 70].

We thank Aleksandr E. Svetogorov for helpful discussions. D.C.O. and W.B. acknowledge support by the Deutsche Forschungsgemeinschaft (DFG; German Research Foundation) via SFB 1432 (Project No. 425217212). F.N. acknowledges support from the European Research Council (grant number 804273) and the Swiss National Science Foundation (grant number 200021\_201082). J.J.G.E. and J.C.C. were supported by the Spanish Ministry of Science and Innovation through a FPU grant (FPU19/05281) and the project No. PID2020-114880GB-I00, respectively, and thank the DFG and SFB 1432 for sponsoring their stay at the University of Konstanz (J.C.C. as a Mercator Fellow).

---

\* david.ohnmacht@uni-konstanz.de

† juancarlos.cuevas@uam.es

- [1] C. W. J. Beenakker and H. van Houten, *Phys. Rev. Lett.* **66**, 3056 (1991).
- [2] A. Furusaki and M. Tsukada, *Phys. Rev. B* **43**, 10164 (1991).
- [3] M. A. Despósito and A. Levy Yeyati, *Phys. Rev. B* **64**, 140511(R) (2001).
- [4] A. Zazunov, V. S. Shumeiko, E. N. Bratus', J. Lantz, and G. Wendin, *Phys. Rev. Lett.* **90**, 087003 (2003).
- [5] N. M. Chtchelkatchev and Yu. V. Nazarov, *Phys. Rev. Lett.* **90**, 226806 (2003).
- [6] C. Padurariu and Yu. V. Nazarov, *Phys. Rev. B* **81**, 144519 (2010).
- [7] J.-D. Pillet, C. H. L. Quay, P. Morfin, C. Bena, A. L. Yeyati, and P. Joyez, *Nat. Phys.* **6**, 965 (2010).
- [8] W. Chang, V. E. Manucharyan, T. S. Jespersen, J. Nygård, and C. M. Marcus, *Phys. Rev. Lett.* **110**, 217005 (2013).
- [9] L. Bretheau, Ç. Ö. Girit, H. Pothier, D. Esteve, and C. Urbina, *Nature* **499**, 312 (2013).
- [10] L. Bretheau, Ç. Ö. Girit, C. Urbina, D. Esteve, and H. Pothier, *Phys. Rev. X* **3**, 041034 (2013).
- [11] C. Janvier, L. Tosi, L. Bretheau, Ç. Ö. Girit, M. Stern, P. Bertet, P. Joyez, D. Vion, D. Esteve, M. F. Goffman, H. Pothier, and C. Urbina, *Science* **349**, 1199 (2015).
- [12] L. Bretheau, J. I.-J. Wang, R. Pisoni, K. Watanabe, T. Taniguchi, and P. Jarillo-Herrero, *Nat. Phys.* **13**, 756 (2017).
- [13] D. J. van Woerkom, A. Proutski, B. van Heck, D. Bouman, J. I. Väyrynen, L. I. Glazman, P. Krogstrup, J. Nygård, L. P. Kouwenhoven, and A. Geresdi, *Nat. Phys.* **13**, 876 (2017).
- [14] M. Hays, G. de Lange, K. Serniak, D. J. van Woerkom, D. Bouman, P. Krogstrup, J. Nygård, A. Geresdi, and M. H. Devoret, *Phys. Rev. Lett.* **121**, 047001 (2018).
- [15] L. Tosi, C. Metzger, M. F. Goffman, C. Urbina, H. Pothier, S. Park, A. L. Yeyati, J. Nygård, and P. Krogstrup, *Phys. Rev. X* **9**, 011010 (2019).
- [16] F. Nichele, E. Portolés, A. Fornieri, A. M. Whiticar, A. C. C. Drachmann, S. Gronin, T. Wang, G. C. Gardner, C. Thomas, A. T. Hatke, M. J. Manfra, and C. M. Marcus, *Phys. Rev. Lett.* **124**, 226801 (2020).
- [17] M. Hays, V. Fatemi, K. Serniak, D. Bouman, S. Diamond, G. de Lange, P. Krogstrup, J. Nygård, A. Geresdi, and M. H. Devoret, *Nat. Phys.* **16**, 1103 (2020).
- [18] M. Hays, V. Fatemi, D. Bouman, J. Cerrillo, S. Diamond, K. Serniak, T. Connolly, P. Krogstrup, J. Nygård, A. Levy Yeyati, A. Geresdi, and M. H. Devoret, *Science* **373**, 430 (2021).
- [19] M. Pita-Vidal, A. Bargerbos, R. Žitko, L. J. Splitthoff, L. Grünhaupt, J. J. Wesdorp, Y. Liu, L. P. Kouwenhoven, R. Aguado, B. van Heck, A. Kou, and C. K. Andersen, *Nat. Phys.* **19**, 1110 (2023).
- [20] M. Hinderling, D. Sabonis, S. Paredes, D. Z. Haxell, M. Coraiola, S. C. ten Kate, E. Cheah, F. Krizek, R. Schott, W. Wegscheider, and F. Nichele, *Phys. Rev. Appl.* **19**, 054026 (2023).
- [21] J. J. Wesdorp, F. J. Matute-Cañadas, A. Vaartjes, L. Grünhaupt, T. Laeven, S. Roelofs, L. J. Splitthoff, M. Pita-Vidal, A. Bargerbos, D. J. van Woerkom, P. Krogstrup, L. P. Kouwenhoven, C. K. Andersen, A. L. Yeyati, B. van Heck, and G. de Lange, *Phys. Rev. B* (2023), arXiv:2208.11198.
- [22] T. Yokoyama and Y. V. Nazarov, *Phys. Rev. B* **92**, 155437 (2015).
- [23] R.-P. Riwar, M. Houzet, J. S. Meyer, and Y. V. Nazarov, *Nat. Commun.* **7**, 11167 (2016).
- [24] E. Eriksson, R.-P. Riwar, M. Houzet, J. S. Meyer, and Y. V. Nazarov, *Phys. Rev. B* **95**, 075417 (2017).
- [25] J. S. Meyer and M. Houzet, *Phys. Rev. Lett.* **119**, 136807 (2017).
- [26] H.-Y. Xie, M. G. Vavilov, and A. Levchenko, *Phys. Rev. B* **96**, 161406(R) (2017).
- [27] H.-Y. Xie and A. Levchenko, *Phys. Rev. B* **99**, 094519 (2019).
- [28] E. V. Repin, Y. Chen, and Y. V. Nazarov, *Phys. Rev. B* **99**, 165414 (2019).
- [29] L. Peralta Gavensky, G. Usaj, and C. A. Balseiro, *Phys. Rev. B* **100**, 014514 (2019).
- [30] M. Houzet and J. S. Meyer, *Phys. Rev. B* **100**, 014521 (2019).
- [31] R. L. Klees, G. Rastelli, J. C. Cuevas, and W. Belzig, *Phys. Rev. Lett.* **124**, 197002 (2020).
- [32] H. Weisbrich, R. L. Klees, G. Rastelli, and W. Belzig, *PRX Quantum* **2**, 010310 (2021).
- [33] H.-Y. Xie, J. Hasan, and A. Levchenko, *Phys. Rev. B* **105**, L241404 (2022).
- [34] H. Barakov and Y. V. Nazarov, *Phys. Rev. B* **107**, 014507 (2023).
- [35] L. Teshler, H. Weisbrich, J. Sturm, R. L. Klees, G. Rastelli, and W. Belzig, Ground state topology of a four-terminal superconducting double quantum dot (2023), arxiv:2304.11982 [cond-mat].
- [36] J. C. Cuevas and H. Pothier, *Phys. Rev. B* **75**, 174513 (2007).
- [37] A. Freyn, B. Douçot, D. Feinberg, and R. Mélin, *Phys. Rev. Lett.* **106**, 257005 (2011).
- [38] T. Jonckheere, J. Rech, T. Martin, B. Douçot, D. Feinberg, and R. Mélin, *Phys. Rev. B* **87**, 214501 (2013).
- [39] R. Mélin, M. Sotito, D. Feinberg, J.-G. Caputo, and B. Douçot, *Phys. Rev. B* **93**, 115436 (2016).
- [40] R. Mélin, J.-G. Caputo, K. Yang, and B. Douçot, *Phys. Rev. B* **95**, 085415 (2017).
- [41] R. Mélin, R. Danneau, K. Yang, J.-G. Caputo, and B. Douçot, *Phys. Rev. B* **100**, 035450 (2019).
- [42] R. Jacquet, A. Popoff, K.-I. Imura, J. Rech, T. Jonck-

- heere, L. Raymond, A. Zazunov, and T. Martin, *Phys. Rev. B* **102**, 064510 (2020).
- [43] B. Douçot, R. Danneau, K. Yang, J.-G. Caputo, and R. Mélin, *Phys. Rev. B* **101**, 035411 (2020).
- [44] R. Mélin, *Phys. Rev. B* **102**, 245435 (2020).
- [45] R. Mélin and B. Douçot, *Phys. Rev. B* **102**, 245436 (2020).
- [46] R. Mélin, *Phys. Rev. B* **104**, 075402 (2021).
- [47] R. Mélin, *Phys. Rev. B* **105**, 155418 (2022).
- [48] R. Mélin and D. Feinberg, *Phys. Rev. B* **107**, L161405 (2023).
- [49] D. Feinberg, T. Jonckheere, J. Rech, T. Martin, B. Douçot, and R. Mélin, *Eur. Phys. J. B* **88**, 99 (2015).
- [50] R. Mélin, R. Danneau, and C. B. Winkelmann, *Phys. Rev. Res.* **5**, 033124 (2023).
- [51] A. H. Pfeffer, J. E. Duvauchelle, H. Courtois, R. Mélin, D. Feinberg, and F. Lefloch, *Phys. Rev. B* **90**, 075401 (2014).
- [52] Y. Cohen, Y. Ronen, J.-H. Kang, M. Heiblum, D. Feinberg, R. Mélin, and H. Shtrikman, *Proc. Natl. Acad. Sci. U.S.A.* **115**, 6991 (2018).
- [53] K.-F. Huang, Y. Ronen, R. Mélin, D. Feinberg, K. Watanabe, T. Taniguchi, and P. Kim, *Nat. Commun.* **13**, 3032 (2022).
- [54] E. G. Arnault, S. Idris, A. McConnell, L. Zhao, T. F. Larson, K. Watanabe, T. Taniguchi, G. Finkelstein, and F. Amet, *Nano Lett.* **22**, 7073 (2022).
- [55] A. W. Draelos, M.-T. Wei, A. Serebinski, H. Li, Y. Mehta, K. Watanabe, T. Taniguchi, I. V. Borzenets, F. Amet, and G. Finkelstein, *Nano Lett.* **19**, 1039 (2019).
- [56] G. V. Graziano, J. S. Lee, M. Pendharkar, C. J. Palmstrøm, and V. S. Pribiag, *Phys. Rev. B* **101**, 054510 (2020).
- [57] N. Pankratova, H. Lee, R. Kuzmin, K. Wickramasinghe, W. Mayer, J. Yuan, M. G. Vavilov, J. Shabani, and V. E. Manucharyan, *Phys. Rev. X* **10**, 031051 (2020).
- [58] E. G. Arnault, T. F. Q. Larson, A. Serebinski, L. Zhao, S. Idris, A. McConnell, K. Watanabe, T. Taniguchi, I. Borzenets, F. Amet, and G. Finkelstein, *Nano Lett.* **21**, 9668 (2021).
- [59] S. Matsuo, J. S. Lee, C.-Y. Chang, Y. Sato, K. Ueda, C. J. Palmstrøm, and S. Tarucha, *Commun. Phys.* **5**, 1 (2022).
- [60] F. Zhang, A. S. Rashid, M. T. Ahari, W. Zhang, K. M. Ananthanarayanan, R. Xiao, G. J. de Coster, M. J. Gilbert, N. Samarth, and M. Kayyalha, *Phys. Rev. B* **107**, L140503 (2023).
- [61] J.-D. Pillet, V. Benzoni, J. Griesmar, J.-L. Smirr, and Ç. Ö. Girit, *Nano Lett.* **19**, 7138 (2019).
- [62] V. Kornich, H. S. Barakov, and Y. V. Nazarov, *Phys. Rev. Res.* **1**, 033004 (2019).
- [63] V. Kornich, H. S. Barakov, and Y. V. Nazarov, *Phys. Rev. B* **101**, 195430 (2020).
- [64] J.-D. Pillet, V. Benzoni, J. Griesmar, J.-L. Smirr, and Ç. Girit, *SciPost Phys. Core* **2**, 009 (2020).
- [65] D. Z. Haxell, M. Coraiola, M. Hinderling, S. C. Ten Kate, D. Sabonis, A. E. Svetogorov, W. Belzig, E. Cheah, F. Krizek, R. Schott, W. Wegscheider, and F. Nichele, *Nano Lett.* **23**, 7532 (2023).
- [66] S. Matsuo, T. Imoto, T. Yokoyama, Y. Sato, T. Lindemann, S. Gronin, G. C. Gardner, M. J. Manfra, and S. Tarucha, Engineering of anomalous Josephson effect in coherently coupled Josephson junctions (2023), arxiv:2305.06596 [cond-mat].
- [67] M. Coraiola, D. Z. Haxell, D. Sabonis, H. Weisbrich, A. E. Svetogorov, M. Hinderling, S. C. ten Kate, E. Cheah, F. Krizek, R. Schott, W. Wegscheider, J. C. Cuevas, W. Belzig, and F. Nichele, *Nat. Commun.* **14**, 6784 (2023).
- [68] See Supplemental Material at ... for details on the calculation of the supercurrent in the single- and double-dot models discussed in the main text. We also provide detailed information on how the ABS spectrum was reconstructed from the experimental data of Ref. [67] and illustrate the robustness of the quartet tomography.
- [69] B. van Heck, S. Mi, and A. R. Akhmerov, *Phys. Rev. B* **90**, 155450 (2014).
- [70] M. Coraiola, D. Z. Haxell, D. Sabonis, M. Hinderling, S. C. ten Kate, E. Cheah, F. Krizek, R. Schott, W. Wegscheider, and F. Nichele, Spin-degeneracy breaking and parity transitions in three-terminal Josephson junctions (2023), arxiv:2307.06715 [cond-mat].